

Structure Dependence of NO Adsorption and Dissociation on Platinum Surfaces

Q. Ge† and M. Neurock*

Contribution from the Department of Chemical Engineering, University of Virginia, Charlottesville, Virginia 22903

Received June 9, 2003; E-mail: mn4n@virginia.edu

Abstract: The influence of surface structure on NO chemisorption and dissociation on Pt{100}-(1×1), Pt{211}, and Pt{410} has been studied using density functional theory slab calculations with the generalized gradient corrections. The presence of steps on Pt{211} strengthens the NO–surface chemisorption bond, but the barrier for NO dissociation remains high. On the other hand, the steps on Pt{410} help to stabilize the N and O adatoms that form upon dissociation and the transition state. The calculated barrier of 80.2 kJ/mol on Pt{410} is in good agreement with experiment. These results show that both the presence of steps and the nature of the steps are important to activate NO. An ensemble of square-arranged Pt atoms has been identified as an important feature in activating the N–O bond.

1. Introduction

It is well recognized that metal surfaces not only provide a template for reaction to proceed but also actively participate in the surface reaction. The role of structural “defects” in heterogeneous reactions has been studied both experimentally and theoretically. It is difficult, however, to quantify their effects in practice because of the random nature of these defects. There is abundant experimental evidence from UHV surface science as well as theoretical studies that indicates adsorbed atoms on transition metals are held stronger at the more open surfaces as well as step and kink sites than on the terrace sites. These high-binding energy sites have been shown to have superior catalytic activity for reactions involving bond-breaking processes. It has been well documented that the bond breaking of adsorbed molecules shifts to lower temperatures on rough and more open surfaces.^{1,2}

The catalytic reduction of NO_x is one of the important reactions that take place in the three-way catalyst,³ which contains platinum. Although alternative pathways such as NO coupling were suggested,^{3,4} the dissociation of NO over the surface is believed to be an important step in this reduction.⁵ As such, the adsorption and dissociation of NO have attracted great attention. In the earlier 1980s, Masel et al. studied a series of platinum stepped surfaces for NO dissociation and found that this reaction was strongly dependent on the surface structure.^{6–18}

The {111} surface was found to be essentially inactive. The {410} surface, on the other hand, was shown to have significantly higher reactivity for NO decomposition. More than 90% of the NO dosed onto the surface was dissociated. N₂ desorption from NO-dosed Pt{410} surface was found to follow simple second-order kinetics,⁸ with an activation energy of 75.4 kJ/mol and preexponential of $3 \times 10^{-2} \text{ cm}^2 \text{ s}^{-1}$. The saturation coverage of NO at room temperature was found to be about half that of CO on the same surface, suggesting that NO occupies up to two sites. Banholzer and Masel tried to rationalize their results on the basis of the orbital symmetry conservation model.⁸ This is analogous to the Woodward–Hoffmann rule, which has been widely used to explain organic and inorganic reactions.¹⁹ For NO activation, electrons are transferred from the σ and π orbitals of the NO molecule to the metal d bands, while the d electrons are transferred to the σ^* and π^* orbitals of the molecule. The symmetry of the metal d orbitals of the surface was believed to determine the reactivity of a particular surface. A comparison of NO decomposition on Pt{210} and {410} showed that the {410} surface is considerably more active than {210} for this reaction, although the geometry of the steps is identical on the two surfaces and the step density is even higher on the {210} surface.¹⁵ Therefore, it seems that NO

† Present address: Department of Chemistry and Biochemistry, Southern Illinois University, Carbondale, IL 62901.

(1) Somorjai, G. A. *Introduction to Surface Chemistry and Catalysis*; Wiley: New York, 1994.
(2) Masel, R. I. *Principles of Adsorption and Reaction on Solid Surfaces*; Wiley: New York, 1996.
(3) Shelef, M.; Graham, G. W. *Catal. Rev. Sci. Eng.* **1994**, *85*, 433.
(4) Bogicevic, A.; Hass, K. C. *Surf. Sci.* **2002**, *506*, L237–242.
(5) Campbell, C. T.; White, J. M. *Appl. Surf. Sci.* **1978**, *1*, 347.
(6) Banholzer, W. F.; Park, Y. O.; Mak, K. M.; Masel, R. I. *Surf. Sci.* **1983**, *128*, 176–190.
(7) Park, Y. O.; Masel, R. I.; Stolt, K. *Surf. Sci.* **1983**, *131*, L385–L389.
(8) Banholzer, W. F.; Masel, R. I. *J. Catal.* **1984**, *85*, 127–134.

(9) Banholzer, W. F.; Masel, R. I. *Surf. Sci.* **1984**, *137*, 339–360.
(10) Masel, R. I. *Surf. Sci.* **1984**, *141*, L331–L337.
(11) Park, Y. O.; Banholzer, W. F.; Masel, R. I. *Appl. Surf. Sci.* **1984**, *19*, 145–160.
(12) Park, Y. O.; Banholzer, W. F.; Masel, R. I. *Surf. Sci.* **1985**, *155*, 341–365.
(13) Banholzer, W. F.; Gohndrone, J. M.; Hatzikos, G. H.; Lang, J. F.; Masel, R. I.; Park, Y. O.; Stolt, K. *J. Vac. Sci. Technol. A-Vac. Surf. Films* **1985**, *3*, 1559–1560.
(14) Banholzer, W. F.; Parise, R. E.; Masel, R. I. *Surf. Sci.* **1985**, *155*, 653–666.
(15) Gohndrone, J. M.; Park, Y. O.; Masel, R. I. *J. Catal.* **1985**, *95*, 244–248.
(16) Lang, J. F.; Masel, R. I. *Surf. Sci.* **1986**, *167*, 261–270.
(17) Masel, R. I. *Catal. Rev.-Sci. Eng.* **1986**, *28*, 335–369.
(18) Gohndrone, J. M.; Masel, R. I. *Surf. Sci.* **1989**, *209*, 44–56.
(19) Woodward, R. B.; Hoffmann, R. *The Conservation of Orbital Symmetry*; Verlag Chemie, GmbH: Deerfield, FL, 1970.

decomposition is sensitive to not only the steps but also the arrangement of the atoms in the step.

Hammer and co-workers reported a number of density functional theory studies of NO dissociation on stepped Pd and Ru surfaces.^{20–25} The stepped Pd{211} has been found to enhance the reactivity only marginally, reducing the NO dissociation barrier from 219 kJ/mol on Pd{111} to 193 kJ/mol on Pd{211}.^{20,21} In contrast, steps artificially created on the Ru{0001} surface have been found to increase the reactivity toward NO dissociation dramatically. The reaction barrier is decreased from 123.5 kJ/mol on the flat surface to 14.5 kJ/mol on the stepped surface.^{22,23}

In the present study, we study the structure sensitivity of Pt by examining the adsorption and dissociation of NO on three structurally different Pt surfaces: {100}, {211}, and {410}. We show that it is not enough only having steps: the local geometrical structure plays an important role in determining the reactivity of a surface.

2. Calculations

Total energy pseudopotential calculations were performed within the framework of density functional theory using a basis set consisting of plane waves.^{26–28} It has been well established that NO loses its spin identity on the Pt surface.²⁹ Therefore, a spin-restricted formalism was adopted in the present calculation. Ultrasoft pseudopotentials with a cutoff energy of 320 eV were used to describe electron–ion interaction in the calculation. The exchange and correlation energies are calculated with the Perdew–Wang form of the generalized gradient approximation (GGA).³⁰ A second-order Methfessel–Paxton smearing³¹ with a width of 0.2 eV was used, and the total energy was extrapolated to 0 K.

The surfaces are modeled using a slab inside a supercell. The GGA-calculated lattice constant of 3.99 Å for Pt was used in the calculations to construct the slabs. Throughout our calculations, we adopted the one-sided slab approach, i.e., placing the adsorbate on one side of the slab and allowing the atoms in the top layers of the slab along with the adsorbate to relax. This approach has been shown to adequately describe many molecule–surface systems.³² The structural details of the slab for the {100}, {211}, and {410} surface will be described in the corresponding sections. Frequency analyses have been performed for some of the adsorption configurations and transition states.

3. Results and Discussion

3.1. NO on Pt{100}-(1×1). The bulk terminated Pt{100} surface is metastable and will reconstruct to a more stable phase in which the surface layer atoms form a quasi-hexagonal structure. This quasi-hexagonal reconstruction can be lifted by adsorption of various adsorbates, such as CO, NO, O₂, and ethylene.³³ It has been suggested that the surface reconstruction is the driving force of the oscillatory behavior of CO oxidation

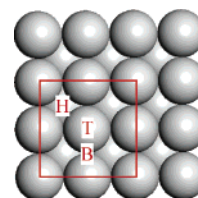


Figure 1. Schematics of Pt{100}-(1×1) with the surface unit cell used in the calculations: T, B, H represent the possible adsorption sites for NO.

Table 1. GGA Adsorption Energies and Structures of NO on Pt{100}-(1×1) and Changes in Averaged First- and Second-Layer Spacing and Corrugations in the First and Second Layer

	bridge			
	atop	upright	parallel	hollow
E_{ads} (kJ/mol)	−136.6	−214.4	−166.5	−157.8
$d_{\text{N-O}}$ (Å)	1.179	1.205	1.234	1.220
$d_{\text{N-Pt}}$ (Å)	1.818	1.983	1.911 (2.170) ^a	2.314
$(\bar{d}_{12}-d)/d$ (%)	−2.3	0.0	−0.8	0.3
δ_1 (Å)	0.29	0.20	0.23	0.0
$(\bar{d}_{23}-d)/d$ (%)	−1.1	−0.4	−1.2	−0.2
δ_2 (Å)	0.0	0.02	0.0	0.14

^a O–Pt bond length, $d_{\text{O-Pt}}$, for this configuration.

Table 2. GGA Adsorption Energies and Structures of N and O Adatoms on Pt{100}-(1×1) and Changes in Averaged First- and Second-Layer Spacing and Corrugations in the First and Second Layer

	N		O	
	bridge	hollow	bridge	hollow
E_{ads} (kJ/mol)	−77.1	−65.8	−109.3	−74.6
bond length (Å)	1.866	2.124	1.961	2.237
$(\bar{d}_{12}-d)/d$ (%)	0.0	2.4	−0.8	0.0
δ_1 (Å)	0.20	0.0	0.17	0.0
$(\bar{d}_{23}-d)/d$ (%)	−0.7	−0.1	−0.9	0.2
δ_2 (Å)	0.05	0.23	0.02	0.21

on this surface.³⁴ The reconstructed quasi-hexagonal surface phase has a very low reactivity, and here we examine only NO adsorption and dissociation on the (1×1) surface phase.

A slab containing four layers of platinum atoms with a vacuum equivalent of six layers of platinum, ~ 12 Å, was used in our calculations for NO adsorption and dissociation on Pt{100}-(1×1). Figure 1 shows a schematic top view of the surface and the (2×2) surface unit cell used in the calculation. The high-symmetry sites for adsorption are also labeled in the figure.

In Table 1 we list the adsorption energy and structure of NO on all these sites at 0.25 ML coverage, corresponding to one NO molecule per surface unit cell. The adsorption energies and structures for O and N adatoms are compiled in Table 2. These results show clearly that NO and atomic O favor the bridge sites, while atomic N prefers the hollow site. In the bridge site, NO adsorbed with its molecular axis normal to the surface is the most favorable configuration, with an adsorption energy of 214.4 kJ/mol. Our present results are in good agreement with previous reported DFT calculations by Ge et al.³⁵ and Eichler and Hafner.^{36,37} In addition, we find that NO can also be strongly adsorbed in a bridge configuration with the N–O molecular

(20) Hammer, B.; Nørskov, J. K. *Phys. Rev. Lett.* **1997**, *79*, 4441–4444.

(21) Hammer, B. *Faraday Discuss.* **1998**, pp 323–333.

(22) Hammer, B. *Phys. Rev. Lett.* **1999**, *83*, 3681–3684.

(23) Hammer, B. *Surf. Sci.* **2000**, *459*, 323–348.

(24) Hammer, B. *Phys. Rev. B* **2001**, *63*, 5423.

(25) Hammer, B. *J. Catal.* **2001**, *199*, 171–176.

(26) Payne, M. C.; Teter, M. P.; Allan, D. C.; Arias, T. A.; Joannopoulos, J. D. *Rev. Mod. Phys.* **1992**, *64*, 1045–1097.

(27) Kresse, G.; Furthmüller, J. *Phys. Rev. B* **1996**, *54*, 11169.

(28) Kresse, G.; Furthmüller, J. *Comput. Mater. Sci.* **1996**, *6*, 15.

(29) Ge, Q.; King, D. A. *Chem. Phys. Lett.* **1998**, *285*, 15–20.

(30) Perdew, J. P.; Chevary, J. A.; Vosko, S. H.; Jackson, K. A.; Pederson, M. R.; Singh, D. J.; Fiolhais, C. *Phys. Rev. B* **1992**, *46*, 6671.

(31) Methfessel, M.; Paxton, A. T. *Phys. Rev. B* **1989**, *40*, 3616–3621.

(32) Ge, Q.; Kose, R.; King, D. A. Adsorption Energetics and Bonding from Femtomole Calorimetry and from First Principles Theory. In *Advances in Catalysis*; Academic Press: San Diego, 2000; Vol. 45, pp 207–260.

(33) Brown, W. A.; Kose, R.; King, D. A. *Chem. Rev.* **1998**, *98*, 797.

(34) Gruyters, M.; King, D. A. *J. Chem. Soc., Faraday Trans.* **1997**, *93*, 2947.

(35) Ge, Q.; Hu, P.; King, D. A.; Lee, M. H.; White, J. A.; Payne, M. C. *J. Chem. Phys.* **1997**, *106*, 1210–1215.

(36) Eichler, A.; Hafner, J. *J. Catal.* **2001**, *204*, 118–128.

(37) Eichler, A.; Hafner, J. *Chem. Phys. Lett.* **2001**, *343*, 383–389.

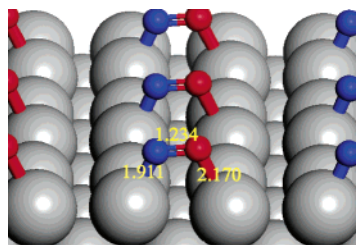


Figure 2. Structure of the “side-on” NO at the bridge sites on Pt{100}.

axis almost parallel to the surface, the “side-on” configuration. The adsorption energy of NO in this configuration is 166.5 kJ/mol. To be certain that the side-on geometry is a true *local* minimum, we distorted the relaxed structure slightly by rotating and displacing the NO molecular axis while maintaining NO at the same height above the surface. These distortions break the 2-fold symmetry and should allow NO to escape from this configuration if it was trapped because of the symmetry constraint. The full relaxations starting from these distorted geometries lead to the same final configuration, indicating that this state was indeed a true local minimum. Figure 2 shows the detailed structural parameters of NO in this lying down adsorption mode.

Normal-mode frequencies for NO at this configuration were calculated by diagonalizing the Hessian matrix from finite displacement calculations. All the frequencies involving NO and surface Pt atoms are real, further confirming that this configuration is indeed a local minimum. The N–O stretching frequency at this configuration is calculated to be 1339 cm^{-1} , compared with 1601 cm^{-1} for NO in the most stable upright bridge configuration. Although the observation of the side-on adsorbed NO species on Pt{100} has not been reported experimentally, it has been suggested on Rh{100} on the basis of results from high-resolution electron energy loss spectroscopy³⁸ and on Ni{100} on the basis of results from X-ray and ultraviolet photoelectron spectroscopies.³⁹ Loffreda et al.⁴⁰ have shown recently that the center of the “lying down” NO on Rh{100} is above the hollow site with the molecular axis almost parallel to the surface. The side-on species has been considered to be a precursor or intermediate leading to NO dissociation.⁴¹ The side-on NO species found in the present study is different, as it lies along the bridging Pt atoms. We show later that this NO species is not active for dissociation. A similar configuration was found for NO adsorbed on Rh{110} at the short-bridge site in a recent DFT-GGA study.⁴² These authors reported that adsorbed NO bound in a side-on geometry is about 20 kJ/mol less stable than the most stable upright configuration.⁴²

Adsorption is usually accompanied by substantial relaxation of substrate, and accurately determining the structure of an adsorption system has been one of the main goals of surface science studies. In agreement with the previous study,³⁵ the clean (1×1) surface exhibits strong inward relaxations, by 4.1% and 1.2% for the first and second layer, respectively. Adsorption of NO, N, and O causes the top layer atoms to relax outward. The extent of the relaxation depends on the particular adsorption

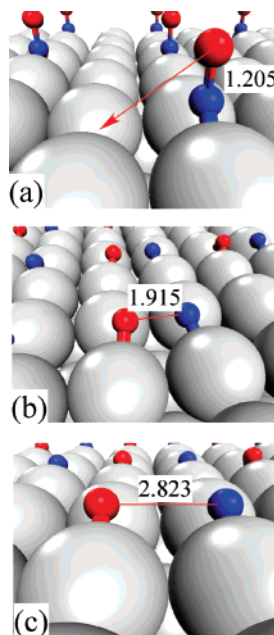


Figure 3. Images of NO dissociation on Pt{100}-(1×1): (a) reactant state; (b) transition state; (c) product state. The N–O distances in all the states are labeled.

site probed and the strength of the chemisorption bond that forms. For example, the adsorption of a N adatom at the hollow site of Pt{100} causes the top layer Pt atoms to relax outward by 2.3% with respect to their bulk terminated positions. The relaxation upon NO and O adsorption, however, only pulls the surface Pt atoms back to their bulk terminated positions. Adsorption at the bridge and atop sites also results in corrugations within the top layers. The extent of this corrugation is tabulated in Tables 1 and 2.

NO dissociation is thought to be the most important step in the NO reduction process. Within a (2×2) surface unit cell, we isolated the transition state for NO dissociation by using the nudged elastic band method.^{43,44} NO starts upright at the bridge site and dissociates into coadsorbed N and O adatoms, with a total coverage of 0.5 ML. The most stable configuration at this coverage is one in which the N and O adatoms occupy parallel bridge sites which sit on opposite sides of the hollow site that lies between them. This elementary step is endothermic, with an overall reaction energy of 86.1 kJ/mol. Along the reaction pathway, the NO molecular axis tilts toward the surface initially. This is followed by stretching of the N–O bond over the hollow site. The coupled translation and rotation modes of the bridge-bonded NO contribute to the initial stage of NO activation. Figure 3 shows the images of the reactant, transition, and product state for this elementary step. This reaction is characterized by a late transition state, whereby the N–O bond is stretched from 1.205 to 1.915 Å. The barrier of this dissociation path is calculated to be 93 kJ/mol, in agreement with the value by Eichler and Hafner.³⁷

We also explored the possibilities of dissociating NO from the side-on configuration. The path that involves NO dissociation to the neighboring bridge site over an atop Pt atom can be ruled out on the basis of the larger energy difference between the immediate product state, coadsorbed N and O adatoms in the

(38) Villarrubia, J. S.; Ho, W. *J. Chem. Phys.* **1987**, *87*, 750.

(39) Sandell, A.; Nilsson, A.; Martensson, N. *Surf. Sci.* **1991**, *241*, L1.

(40) Loffreda, D.; Delbecq, F.; Simon, D.; Sautet, P. *J. Chem. Phys.* **2001**, *115*, 8101–8111.

(41) Gu, J.; Yeo, Y. Y.; Miao, L.; King, D. A. *Surf. Sci.* **2000**, *464*, 68–82.

(42) Liao, D.; Glassford, K. M.; Ramprasad, R.; Adams, J. B. *Surf. Sci.* **1998**, *415*, 11–19.

(43) Ulitsky, A.; Elber, R. *J. Phys. Chem.* **1990**, *92*, 1510–1511.

(44) Mills, G.; Jónsson, H.; Schenter, G. K. *Surf. Sci.* **1995**, *324*, 305.

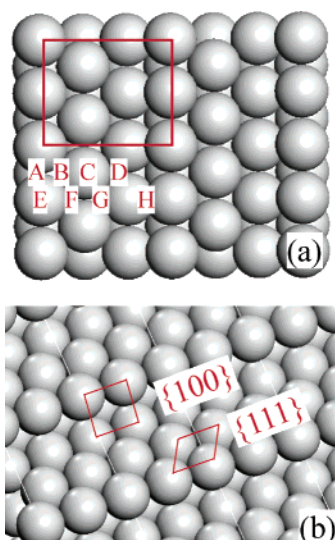


Figure 4. Schematics of a Pt{211} surface, with (a) top view with the surface unit cell used and adsorption sites examined; (b) perspective view showing the {111} terrace and {100} step.

bridge sites of the same Pt row. This energy difference is 142.6 kJ/mol, significantly higher than the dissociation barrier over the hollow site to the opposite bridge site of the next Pt row. An alternative path involves NO activation over the neighboring bridge site of the perpendicular Pt rows. This pathway was calculated to have a barrier of 136.7 kJ/mol. Furthermore, we would point out that both the reaction energy and activation barrier for this configuration were calculated with respect to the energy of the side-on adsorption mode. If the energy to activate NO from the most stable upright bridge configuration were taken into account, the overall energy cost and reaction barrier would be even higher. A third possibility is that NO rolls over to the hollow site. Along this pathway, NO dissociates via a transition state that is similar to the one shown in Figure 3b. However, NO would have to overcome a barrier to reach this state, as the side-on configuration is a local minimum. The path through the side-on adsorption mode as a precursor for NO dissociation is therefore at least as high as that from the bridge-bonded NO. The most favorable pathway is that where NO dissociates across the 4-fold hollow site with no metal atom sharing between the N and O adatoms that form on the surface. This acts to remove the repulsive interactions that exist when two dissociating fragments share metal atoms.⁴⁵ The removal of the repulsive interactions helps to stabilize the transition state and lower the reaction barrier.

3.2. NO on Pt{211}. Pt{211} consists of three atom wide {111}-type terraces and {100}-type single atom steps. The low symmetry of the stepped surface opens up more sites where NO as well as its dissociative products, N and O adatoms, can be adsorbed. The surface unit cell as well as the possible adsorption sites examined are shown in Figure 4a. For clarity, we present a schematic view of the surface showing the steps in Figure 4b. The slab consist of 12 {211} layers, which is equivalent to four {111} layers. We will discuss adsorption and dissociation in turn in the remainder of the section.

3.2.1. Adsorption. We first examined a series of adsorption sites along the $\langle 111 \rangle$ direction on the surface. In particular, two

Table 3. GGA Adsorption Energies and Structures of Chemisorbed NO on Pt{211}

	E_{ads} (kJ/mol)	$d_{\text{N-O}}$ (Å)	$d_{\text{N-Pt}}$ (Å)	θ
A	-232.1	1.207	1.982	-1.9
A1	-226.6	1.208	1.992	16.3
B	-191.3	1.219	2.096(2), 2.162	14.6
C	-79.1	1.176	1.846	-4.9
D	-131.5	1.230	2.003, 2.105(2)	19.3
E	-168.7	1.177	1.822	2.2
F	-175.9	1.222	2.083, 2.104(2)	12.0
G	-150.6	1.218	2.066(2), 2.149	16.6
H	-170.3	1.205	1.948, 2.009	-31.4

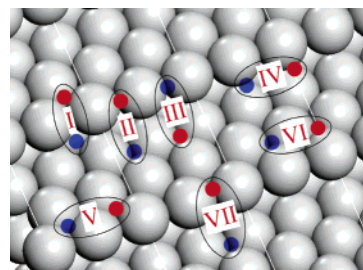


Figure 5. Possible combinations of coadsorbed N and O adatoms on Pt{211} as products of NO dissociation. The blue and red dots represent N and O adatoms, respectively.

high-symmetry planes have been probed: one passes through the bridge sites, while the second passes through the atop sites on the step edge. Table 3 lists the calculated binding energies and bond lengths of N–O and N–Pt at various sites on the {211} surface, as shown in Figure 4a. The polar angle (θ) of the N–O molecular axis with respect to the surface normal is also given in the table. Clearly, the bridge site at the edge of the step is most stable for NO adsorption, with an adsorption energy of -232.1 kJ/mol. This is similar to NO adsorption on the reconstructed (1×2) surface phase of Pt{110}.^{46,47} At this configuration, the NO molecular axis is slightly tilted toward the lower terrace, by $\sim 2^\circ$. We also isolated a minimum for NO at this site but with its molecular axis almost normal to the {111} terrace. The chemisorption bond for NO in this configuration is only slightly weaker than the most stable bridge structure, listed as site A1 in Table 3. This indicates that the coupled translation–rotation of NO in the bridge site on the edge of the step is a very soft mode.

As NO is moved toward the bottom of the step on the {111} terrace, the chemisorption bond between NO and the surface is greatly weakened, as manifested by the decreased adsorption energy, from -191.4 kJ/mol of the hollow site close to the top of the step edge (site B in Figure 4a) to -131.5 kJ/mol of the hollow site at the bottom of the step edges (site D). As a consequence, NO adsorption will be favorable at the top of the step edge, which is in agreement with the expected high reactivity of stepped surfaces for adsorption.

3.2.2. Dissociation. To establish the final state for the NO dissociation pathways over Pt{211}, we computed the combined N and O adsorption energies for the coadsorbed N and O adatoms at different configurations on the surface, as shown in Figure 5. The combined N and O adsorption energies are

(46) Brown, W. A.; Ge, Q.; Sharma, R. K.; King, D. A. *Chem. Phys. Lett.* **1999**, *299*, 253–259.

(47) Ge, Q.; Brown, W. A.; Sharma, R. K.; King, D. A. *J. Chem. Phys.* **1999**, *110*, 12082–12088.

(45) Johnson, K.; Ge, Q.; Titmuss, S.; King, D. A. *J. Chem. Phys.* **2000**, *112*, 10460.

Table 4. GGA Adsorption Energies (with respect to molecular NO) and Structures of Coadsorbed N and O Adatoms on Pt{211}

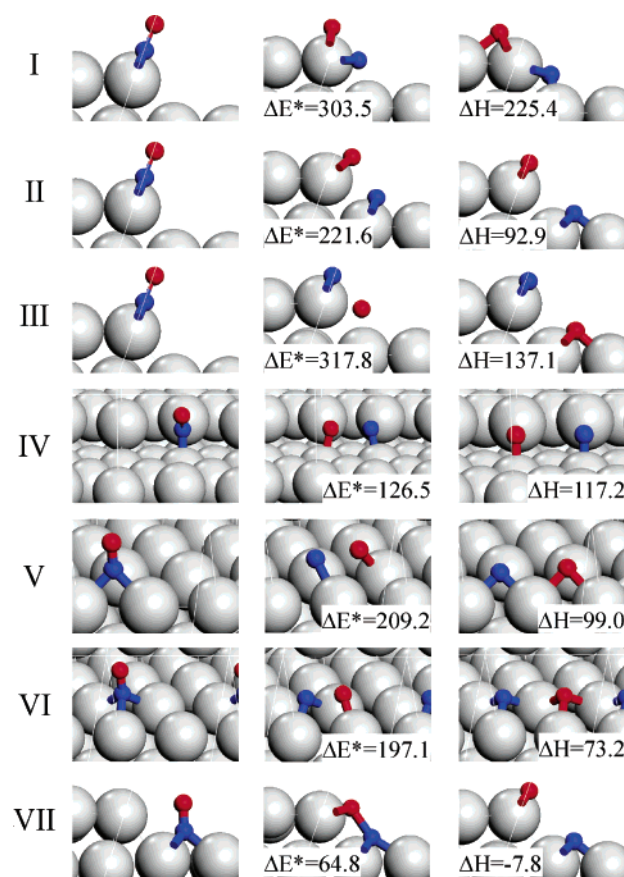
	E_{ads} (kJ/mol)	$d_{\text{N-O}}$ (Å)	$d_{\text{N-Pt}}$ (Å)	$d_{\text{O-Pt}}$ (Å)
I	7.5	2.867	2.122(2), 2.158(2)	2.140, 2.108(2)
II	-139.3	2.911	1.913, 1.969(2)	1.950(2)
III	-95.1	2.957	1.857(2)	2.019, 2.044(2)
IV	-53.1	2.822	1.838, 1.885	1.938, 1.983
V	-92.3	2.830	1.960, 1.956(2)	2.974, 2.093(2)
VI	-102.7	2.826	1.943, 1.970(2)	2.031, 2.099(2)

calculated with respect to the gas phase NO molecule. The energies as well as the structure parameters for different configurations are given in Table 4. These configurations of coadsorbed N and O adatoms are not necessarily the lowest energy combinations but are the direct dissociation products that can form from the corresponding NO adsorption states.

We explored seven possible NO dissociation paths, focusing on the paths that occur in the vicinity of the step. The first path starts from NO chemisorbed in the most stable bridge site on the step edge. As the reaction proceeds, the N-end of the molecule slides down the step slightly while the NO molecular axis rotates inward toward the surface of the upper terrace. The N atom ends up at a pseudo 4-fold site on the {100} step which is formed by the edge atoms of the upper terrace and the atoms at the bottom of the steps and the oxygen atom in the 3-fold site close to the edge of the upper terrace. This reaction is endothermic, with a reaction energy of 225.4 kJ/mol. Correspondingly, the barrier of this reaction pathway is very high, at 303.5 kJ/mol. The N and O adatoms that form in the transition state share the bridging Pt atoms on the step edge, as shown in Figure 6I. This leads a strong repulsive interaction, which is the main reason for the high activation barrier.

The second pathway starts with NO in the same adsorption state as in the first path. In the product state, N is adsorbed in a 3-fold hollow site on the lower terrace while O is bound to the bridge site at the top of the step edge. The overall reaction energy of this path is 92.9 kJ/mol. The path is quite similar to the previous one where the N-end of the molecule slides down the step while NO bends toward the surface. The transition state for this reaction is one in which the N and O adatoms occupy the bridge sites that sit across the pseudo 4-fold site of the {100} step. The barrier of this reaction pathway is 220 kJ/mol, which is lower than the previous pathway but still significantly higher than that over the 4-fold hollow site on the Pt{100} surface. This is due to the fact that although N and O adatoms do not share surface Pt atoms anymore, the Pt atoms at the bottom of the step have 10 Pt neighbors whereas the Pt atoms at the flat {100} surface have only eight neighbors. A higher coordination of the Pt atoms would weaken their interaction with adsorbates and thus increase the barrier for activation over that on the {100} surface.

The third pathway also starts from the same initial state as the previous two paths. However, the N-end of chemisorbed NO does not slide down the step. Instead, the O-end swings toward the lower terrace while the N-end remains at the bridge site on the top of the step edge. The final state for this path is one in which N is chemisorbed at the bridge site at the top of the step edge while O sits in the pseudo 3-fold site on the lower terrace. This path is actually more endothermic than the previous path, with an overall reaction energy of 137.1 kJ/mol. The activation barrier for this path is also higher, at ~317.8 kJ/mol.

**Figure 6.** Seven (I–VII) possible NO dissociation pathways on Pt{211}. The images on the left, middle, and right represent reactant, transition, and product states of the local reaction path. The small blue and red balls represent N and O, respectively. Detailed structure parameters of the final states are given in Table 4.

The fourth pathway starts with NO adsorbed at the bridge site on the {100} step, site H as shown in Figure 4. NO dissociates over the hollow site on the {100} step, similar to that on an ideal {100} surface. This elementary step corresponds to an overall reaction energy of 120.1 kJ/mol and a barrier of 126.5 kJ/mol. These values are higher than but comparable with the reaction and activation energies on the ideal {100} surface, as shown in the previous section. However, it is important to remember that NO adsorbed in site H is 61.9 kJ/mol less stable than NO in the most stable bridge sites on the step edge. Although the barrier for this reaction path appears low, it requires an activation of NO from the most stable bridge site on the upper terrace to the meta-stable bridge site on the {100} step before NO dissociation can proceed along this pathway.

Along the fifth and sixth pathways, NO dissociation occurs along the {111} terrace. The fifth pathway occurs closer to the edge of the terrace than the sixth. The dissociations along these pathways are very similar to that on the Pt{111}. The overall reaction energies are 99.0 and 73.2 kJ/mol and the reaction barriers are 213.8 and 200.4 kJ/mol, for the fifth and sixth pathways, respectively. These values are in agreement with the reaction energy (76.7 kJ/mol) and barrier (210 kJ/mol) that we calculated for NO dissociation over Pt{111}. They are also in good agreement with the activation barriers of 203 and 193 kJ/mol for NO dissociation on the {111} terraces of Pt{533} and Pt{553}, respectively, reported recently by Eichler.⁴⁸ Similarly, we need to take into account the energy differences required to

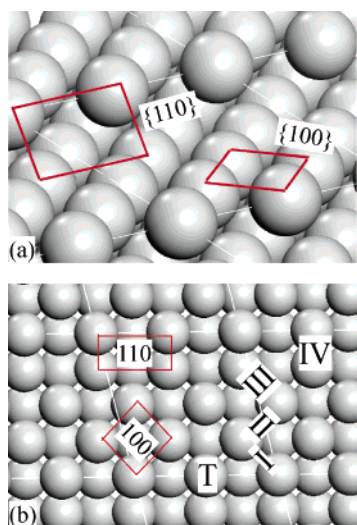


Figure 7. Schematics of the Pt{410} surface: (a) perspective view showing the terraces and the steps; (b) top view showing the unit cell used in the calculation and the NO adsorption sites examined.

populate the initial NO adsorption states for these paths and the most stable NO state when we compare the overall and activation energies of these pathways with those of others.

The seventh and last pathway we examined on this surface is that where NO starts from a hollow site at the bottom of the step, site D. As the reaction proceeds, the molecular axis of NO leans toward the step and the N–O bond begins to stretch. The final state for this path is one in which nitrogen sits in the pseudo 4-fold site on the {100} step and the oxygen in the 3-fold site on the edge of the upper terrace. This is the same product as that found in path II. However, this pathway differs from path II in that its transition state is closer to the lower terrace. The reaction from NO in this state to the coadsorbed N and O atoms state is exothermic, with a reaction barrier of 64.8 kJ/mol. Even if we take the energy difference between the starting NO state and the most stable NO adsorption state, 100.6 kJ/mol, the overall barrier is still the lowest among all the NO dissociation pathways on Pt{211} examined here.

A summary of all seven pathways with the schematic structures and energetics is given in Figure 6. Overall, path VII has the lowest intrinsic barrier, at 64.8 kJ/mol. The intrinsic barrier for path IV is also relatively low. Even if we take into account the energy cost to activate NO from the most stable adsorption site, site A in Figure 4, the effective barriers for these two pathways are still more favorable than the rest of the pathways. All the other five pathways examined here have significantly high intrinsic barrier, more than 200 kJ/mol. A common feature of the two low barrier pathways is that the dissociation takes place over a hollow site of the square-arranged Pt atoms, thus eliminating any metal sharing in the transition state.

3.3. NO on Pt{410}. Pt{410} consists of the {100}-type terraces and the {110}-type single atom steps, as sketched in Figure 7. The {410} cut of the surface is about 11° off the {100} terrace. The main reason for choosing this surface was due to the extraordinary reactivity of this surface exhibited toward NO dissociation, as demonstrated by the ultrahigh-vacuum experimental results.⁸

Table 5. GGA Adsorption Energies and Structures of Chemisorbed NO on Pt{410}^a

	E_{ads} (kJ/mol)	$d_{\text{N-O}}$ (Å)	$d_{\text{N-Pt}}$ (Å)	θ (deg)
I	−216.8	1.208	1.971, 1.994	3.8
II	−210.3	1.208	1.985	4.5
III	−201.0	1.205	1.966, 1.970	0.4
IV	−159.6	1.228	2.007, 2.017	−22.2
T	−196.0	1.186	1.857	25.1

^a See Figure 7 for definition of the sites.

As we showed in the previous section, the existence of a step edge will help to strengthen the NO–surface bond. We will therefore concentrate on the possible dissociation pathways that occur within the vicinity of the step edge rather than thoroughly explore all conceivable NO adsorption and activation sites. From the results of NO on Pt{100}, we learned that NO strongly favors the bridge sites. Therefore, we examined the bridge sites across the {100} terrace from the edge to the bottom of the steps, as depicted in Figure 7.

The calculated adsorption energies for NO at various bridge sites and one atop site are listed in Table 5. Not surprisingly, the results show that the strongest binding occurs at the site close to the step edge, with an adsorption energy of −216.8 kJ/mol. As NO was moved toward the bottom of the step on the {100} terrace, the NO chemisorption bond becomes weaker and the adsorption energy is reduced to −201.0 kJ/mol. The NO adsorption energies at a bridge site in the middle of the {100} terrace is similar to that on the {100} surface, at ca. −210 kJ/mol. The chemisorbed NO at the bridge site of the {110} step between the upper and lower terrace is far less stable. The adsorption energy at this site is only −159.6 kJ/mol. NO in this site is even less stable than the NO at the atop site of the edge Pt atoms. The adsorption energy of the edge-bound atop NO is −196.0 kJ/mol. This adsorption energy is almost as high as that of the bridge-bonded NO. At this atop site, NO is adsorbed in a highly bent geometry. The N–Pt bond axis is tilted toward the lower terrace by 10° from the surface normal, while the N–O bond axis is tilted in the opposite direction toward the upper terrace by 25.1°, leading to $\angle\text{ONPt} = 143.9^\circ$. As NO in this site is primarily coordinated to a single Pt atom, the bond lengths of both the N–Pt and N–O bonds are relatively short, as shown in Table 5.

As shown in the previous section on Pt{100}, the barrier for NO dissociation on the ideal (1×1) structure of the {100} surface is modest, at ~95 kJ/mol. We would expect both the endothermicity and the reaction barrier will be lower on the {410} surface, as the step edge provides extra stabilization for the product states and perhaps the transition state. Several possible reaction pathways were explored in the vicinity of the step. In particular, we examined a possible transition state that is similar to the configuration on the {100} surface, with N–O occupying a 4-fold hollow site close to the step edge and the N–O axis being almost parallel to the {100} terrace. The results of vibrational frequency analysis confirm that this state is a transition state. The activation energy of this transition state with respect to the most stable NO adsorption state is 106 kJ/mol. However, searching with the nudged elastic band method between the initial NO adsorption state and the final N and O coadsorbed state did not lead to this transition state. Instead, the pathway shown in Figure 8 was found to be most favorable. This local reaction path starts from the most stable adsorption

(48) Eichler, A. Personal communication, 2003.

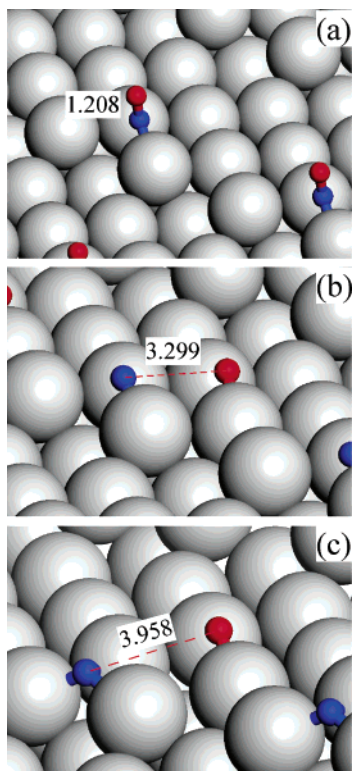


Figure 8. Images of NO dissociation on Pt{410}: (a) reactant geometry; (b) transition state; and (c) product state.

state of NO where NO occupies the bridge site close to the top of the step (site I). The NO molecular axis bends down onto the {100} terrace. The final state for this reaction is that in which N is adsorbed in the hollow site on the step edges while O sits in the bridge site across a 4-fold site. The hollow site that N occupies is formed from a 4-fold site on a {100} surface by removing one of the four corner atoms to create the step. As such, this site is a hollow site that does not exist on a flat surface. Upon N adatom formation at this site, the interactions of Pt atoms with the N adatom deforms this site to a pseudo-3-fold site. This helps to stabilize the product, as manifested by the low overall reaction energy of 31.1 kJ/mol, which is 60 kJ/mol less than that on the ideal {100} surface.

The images for the reactant, transition, and product states for this local path are shown in Figure 8. The barrier for this pathway is calculated to be 80.2 kJ/mol, in good agreement with the experimental value of 75.4 kJ/mol. Similar to that on Pt{100}, NO dissociation takes place over a 4-fold hollow site on the {100} terrace. The transition state again involves Pt atoms with a square arrangement whereby the N and O adatoms that form do not share metal atoms in the transition state. As compared with the transition state on Pt{100}, this transition state occurs even “later” along the reaction coordinate, as is characterized by the increased N–O separation. To be certain that the isolated state was indeed a transition state, we again performed a frequency analysis for the determined transition state. The results, which include the neighboring Pt atoms, showed that there was only one imaginary frequency that corresponded to the N–O stretching mode.

3.4. General Discussions. As we stated earlier, it has been well documented that defect sites such as steps and kinks will enhance the reactivity of a solid surface. We use NO adsorption

and dissociation on ideal Pt{100}-(1×1), Pt{211}, and Pt{410} as model systems to examine the structure-related reactivity. Earlier surface science experiments on single-crystal surfaces show that Pt{100}-(1×1) is the only low-index Pt surface that exhibits moderate reactivity toward NO dissociation.⁴⁹ Pt{111} is essentially inert for NO dissociation, and even the more open {110} surface does not show appreciable reactivity.⁵⁰

As shown in the present study, the steps on Pt{211} do not enhance the reactivity toward NO dissociation, although they indeed strengthen the NO–surface bond. In contrast, the existence of steps on the {410} surface significantly lowers both the overall reaction energy and the reaction barrier. In Figure 9, we plot our DFT-calculated activation energies on top of the structure sensitivity diagram constructed by Masel, which correlates NO dissociation rates as well as activation barriers with the different faces of platinum.² The results show that the DFT-calculated activation energies agree reasonably well with the experimental results.

One common feature on all the surfaces examined here is that the transition states with lowest energy correspond to NO dissociation over a hollow site of square-arranged Pt atoms whereby the N and O adatoms that form are separated over two different bridge sites. This removes metal–atom sharing in the transition state, which significantly lowers repulsive interactions in the transition state.

The N–O distance at all of the transition states examined here is greatly stretched compared with the gas phase NO bond length. The stretched N–O distance at the transition states indicates that the barrier for NO dissociation on all the surfaces is located at the exit channel, i.e., a “late transition state”. Late transition states typically have structural and bonding properties similar to that of the product states. This can be clearly seen in the density of states (DOSs) plot shown in Figure 10. In Figure 10, we plotted the local DOSs of N (a–c) and O (d–f) for starting NO chemisorbed state (a and d), transition state (b and e), and final N and O coadsorbed state (c and f) for NO dissociation on Pt{100}. The similarity for both N and O local DOSs between transition and final states is self-evident. The interactions with the metal atoms are reflected in the broad features between –7.5 eV and the Fermi level, which are the results of the mixing between π (or p) states of NO (N or O atoms) with the metal d states of Pt.

Hammer²² proposed to decompose the transition state potential energy (E_{ts}), the total energy at the transition state with respect to the gas phase NO, into rebonding energy (E_{rebond}) and intramolecular interaction energy (E_{int}) between N and O atoms at the transition states:

$$E_{ts} = E_{rebond} + E_{int}$$

Obviously, both the rebonding and the intramolecular interaction energies depend strongly on the structure of the transition state. We examined the transition states with the lowest energies on each of the surfaces and noted that all the transition states occupied a site with square-arranged Pt atoms. With this arrangement, there is no metal sharing between N and O atoms at the transition state. The interaction energies calculated are 44.7, 47.2, and 43.8 kJ/mol for {410}, {100}, and {211},

(49) Gorte, R. J.; Schmidt, L. D.; Gland, J. L. *Surf. Sci.* **1981**, *109*, 367.

(50) Gorte, R. J.; Gland, J. L. *Surf. Sci.* **1981**, *102*, 348–358.

Structure Sensitivity for NO Decomposition

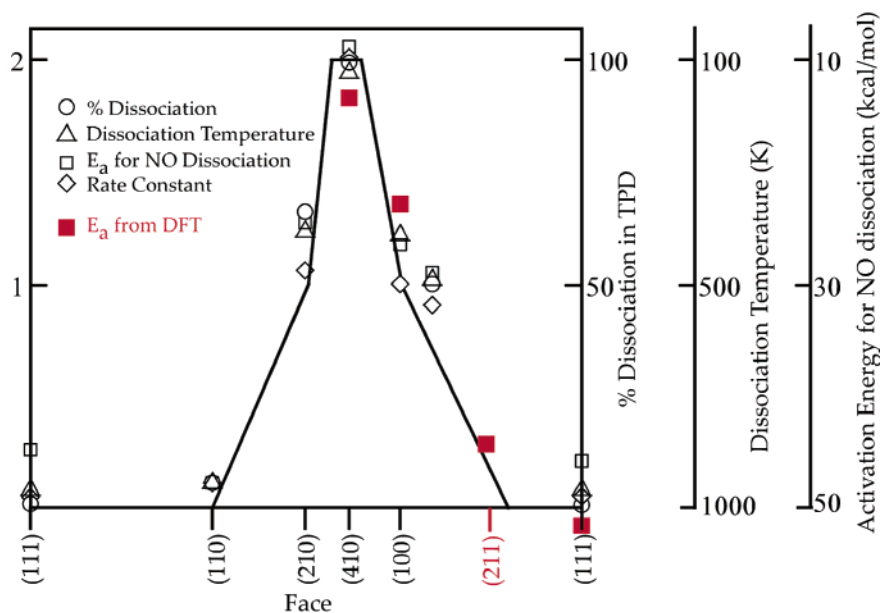


Figure 9. Comparison of the DFT-calculated NO dissociation activation energies for different faces of platinum with experimental results, as shown in the structure sensitivity diagram constructed by Masel, adapted from ref 2 by permission of John Wiley & Sons, Inc. Copyright ©1996.

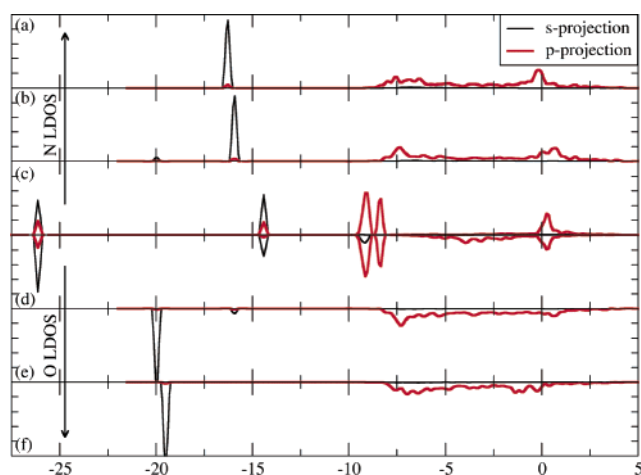


Figure 10. Local density of states of N and O for NO dissociation on Pt{100}. N local DOSs for final state (a), transition state (b), and NO (c); O local DOSs for NO (d), transition state (e), and final state (f).

respectively. The nearly constant intramolecular interaction energies for these paths on different surfaces is another indication that the transition states are of similar structures. According to Hammett,²² the transition state potential, and therefore, the reaction barrier, will be governed by the rebonding energy of N and O at the transition states. A correlation between the activation energy of NO dissociation on the three surfaces is plotted against the rebonding energy in Figure 11. The enhanced reactivity on {410} can be attributed to the increased rebonding potential of N and O at the transition state. Liu and Hu performed similar but slightly different analyses for C–O and C–H bond breaking on a number of metal surfaces.^{51,52} These analyses are in essence the same as the Hammett and Hammond^{53,54} relationships which state that the energies of the

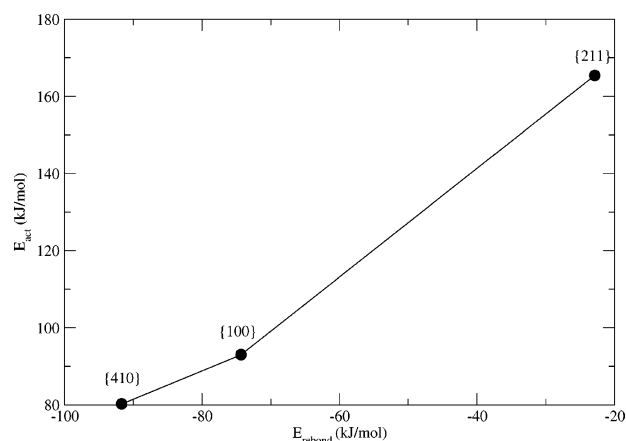


Figure 11. Correlation of NO dissociation barriers on Pt{410}, {100}, and {211} with the rebonding energy of N and O on these surfaces.

product state can be used as a measure of the activation energy for a reaction with a late transition state.

4. Conclusions

We have used the density functional theory total energy method to study NO adsorption and dissociation on the {100}-(1 × 1), {211}, and {410} surfaces of Pt. We demonstrated that both the presence of defects and the local geometry of the defects are important in determining the reactivity of a surface.

The presence of steps on {211} and {410} opens more sites for NO adsorption. Both surfaces show increased reactivity toward NO adsorption at the edge of the steps, manifested by the higher binding energy of NO on these surfaces than on flat surfaces. However the presence of steps on Pt{211} does not increase its reactivity for NO dissociation. NO dissociation on Pt{410} has the lowest barrier among all three surfaces, with an activation energy of 80.2 kJ/mol, in agreement with earlier experiment results.

The dissociation of NO is characterized by a late transition state. The surface atoms with a square arrangement are found

(51) Liu, Z.-P.; Hu, P. *J. Chem. Phys.* **2001**, *114*, 8244.

(52) Liu, Z.-P.; Hu, P. *J. Am. Chem. Soc.* **2003**, *125*, 1958.

(53) Hammett, L. P. *J. Am. Chem. Soc.* **1937**, *59*, 96.

(54) Hammond, G. S. *J. Am. Chem. Soc.* **1955**, *77*, 337.

to form an ensemble that provides the active site for NO dissociation on all three surfaces. The square arrangement of the atoms at the active site produces an environment where metal sharing for N and O adatoms at the transition state is removed, thereby enhancing the rebonding of N and O to the surface.

Acknowledgment. We acknowledge financial support from NovoDynamics Inc. We also thank Dr. Laurent Kieken, Dr. Jan Lerou, and Prof. Enrique Iglesia for valuable discussions; Dr.

Andreas Eichler for sharing his results (ref 48) prior to publication, and Prof. J. Hafner for the use of their VASP code. Calculations were performed in part on Blue Horizon at the San Diego Super Computing Center, Terascale Computer System at Pittsburgh Supercomputing Center, and Centurion nodes at the University of Virginia.

JA036575O